Performance of a scroll compressor working with drop-in refrigerant replacements to R134a

Riccardo CONTE[1], Marco AZZOLIN[1]*, Stefano BERNARDINELLO[2], Davide DEL COL[1]

[1] University of Padova, Department of Industrial Engineering,
Padova, Italy
(marco.azzolin@unipd.it)

[2] Swegon Operations S.r.l,
Cantarana di Cona, Venice, Italy

* Corresponding Author

ABSTRACT

Most of the countries around the world are adopting regulations and actions to reduce the use of hydrofluorocarbon (HFC) refrigerants with high Global Warming Potential (GWP). Among the HFCs, R134a, which has a $GWP_{100years}$ equal to 1530, is recognized by the IPCC as a major contributor and its atmospheric abundance increased by 71 % from 2011 to 2019. This work presents an experimental study on the performance of a new scroll compressor operating with six low-GWP refrigerants as drop-in alternatives to R134a. The refrigerants used are: R1234ze(E), R152a, R516A, R515B, R450A and R513A. The test system is a water-to-water chiller working with two large scroll compressors (swept volume for each compressor equal to 222.5 $m^3\ h^{-1}$) and two brazed plate heat exchangers as the condenser and the evaporator. The experimental tests were conducted by fixing the inlet/outlet water temperatures in the heat exchangers when producing cold water at 7°C and 18°C. The data allow to evaluate and assess the compressor performance in terms of volumetric efficiency and global isentropic efficiency. Numerical correlations of Pierre (1982) and Navarro et al. (2013) to estimate the compressor efficiencies have been compared against the experimental data and new coefficients have been determined for those correlations.

1. INTRODUCTION

The recent proposal of the new F-gas Regulation of the European Commission (EU No 2024/573, 2024), and the Kigali Amendment to the Montreal Protocol on Substances that Deplete the Ozone Layer (2016) are some actions taken to reduce the use of hydrofluorocarbon (HFC) refrigerants with high Global Warming Potential (GWP). The aim is to reduce greenhouse gas emissions in the air-conditioning and refrigeration industry. Among the HFCs, R134a is recognized in the IPCC AR6 as a major contributor and its atmospheric abundances is increased by 71 % from 2011 to 2019 (IPCC, 2022). Therefore, it is urgent to find low-GWP and zero ODP (ozone depletion potential) fluids as substitutes for R134a. Theoretical studies have already been conducted to evaluate the use of non-flammable pure refrigerants or mixtures as an alternative (Bell et al., 2019). Some possible candidates are: R1234ze(E), R152a, R516A, R515B, R450A and R513A. Several works compared the performance of heat pumps or refrigerating systems with R1234ze(E) and R152a as possible replacements for R134a, with different compressor types: reciprocating hermetic-type compressor (Sánchez et al., 2017), reciprocating open-type compressor (Mota-Babiloni et al., 2014) and reciprocating semi-hermetic-type compressor (Colombo et al., 2020). Less work deals with R450A, R513A and R516A. When considering R450A and R513A, they have been studied in system equipment with rotary compressors (Makhnatch et al., 2019; Mota-Babiloni et al., 2017), with semi-hermetic compressors (Llopis et al., 2017) or with reciprocating open-type compressors (Mendoza-Miranda et al., 2016). A vapour compressor system equipment with a scroll compressor has been studied with R513A and R516A as refrigerants (Al-Sayyab et al., 2022).
From this literature review emerges a gap of experimental studies regarding the performance of vapor compression cycles equipped with scroll compressors and working with possible replacements for R134a. The present study aims at contributing to this topic by presenting a water-to-water chiller equipped with two scroll compressors and tested with several alternatives to R134a: R1234ze(E), R152a, R516A, R515B, R450A and R513A. Experimental tests have

been conducted and the results in terms of compressor efficiencies are discussed and compared with the predictions of models of Pierre (1982) and Navarro et al. (2013).

2. MAIN CHARACTERISTIC OF REFRIGERANTS

Table 1 summaries the main properties of the tested refrigerants: three pure fluids (R134a, R1234ze(E) and R152a), two azeotropic blends (R516A and R515B) and two nearly azeotropic blends (R513A and R450A).
Compared to R134a:

- the molar mass of the alternatives is similar or higher, except for R152a. This mainly affects the latent heat of vaporization, which is lower compared to that of R134a;
- all the refrigerants have a lower critical pressure, except for R152a, and thus systems designed for R134a will not suffer from additional pressure stress;
- R516A and R513A have higher vapor densities (+11% and +19% respectively) and this leads to a higher mass flow rate processed by the compressor. The lower vapor density of R1234ze(E), R152a, R515B and R450A leads to a higher specific vapor volume, which reduces the mass flow rate processed by the compressor.

Table 1: Main characteristics of tested refrigerants.

Refrigerant	**R134a**	**R1234ze(E)**	**R152a**	**R516A**	**R515B**	**R513A**	**R450A**
Composition	pure	pure	pure	R134a/R152a/ R1234yf 8.5/14/ 77.5 wt%	R227ea/ R1234ze(E) 8.9/91.1 wt%	R134a/ R1234yf 44/56 wt%	R134a/ R1234ze(E) 42/58 wt%
ASHRAE Safety classification	A1	A2L	A2	A2L	A1	A1	A1
$GWP_{100\text{-}yr}$ [aa]	1530	1.37	164	153	322	673	643
ODP	0	0	0	0	0	0	0
Molar mass (kg $kmol^{-1}$)	102	114	66	103	117	108	109
Critical temperature (°C)	101	109	113	97	109	95	105
Critical pressure (MPa)	4.1	3.6	4.5	3.6	3.6	3.7	3.8
Boiling point at 0.1 MPa (°C)	-26.4	-19.3	-24.3	-29.7	-19.1	-29.9	-23.7
Temperature glide at 0.1 MPa (K)	0	0	0	0	0	0.1	0.6
Latent heat of vaporization [b] (kJ kg^{-1})	199	184	307	184	179	176	189
Liquid density[b] (kg m^{-3})	1295	1240	959	1148	1259	1222	1260
Vapor density[b] (kg m^{-3})	14.4	11.7	8.4	16.0	12.0	17.2	13.2
Liquid specific heat[b] (kJ kg^{-1} K^{-1})	1.34	1.32	1.70	1.35	1.30	1.31	1.33
Vapor specific heat[b] (kJ kg^{-1} K^{-1})	0.90	0.88	1.09	0.95	0.88	0.92	0.89
Liquid thermal conductivity [b] (mW m^{-1} K^{-1})	92.0	83.1	109.0	78.9	81.9	79.2	86.2
Vapor thermal conductivity [b] (mW m^{-1} K^{-1})	11.5	11.6	12.0	12.0	11.8	11.7	11.7
Liquid viscosity [b] (µPa s)	266.5	262.6	219.1	207.8	266.6	224.7	260.3
Vapor viscosity [b] (µPa s)	10.7	10.7	9.2	10.3	10.7	10.6	10.7

3. EXPERIMENTAL SYSTEM AND TEST PROCEDURE

3.1 Experimental system

The experimental tests were conducted in a water-to-water chiller with a nominal cooling capacity equal to 300 kW. Figure 1 illustrates the test bench, which includes three distinct loops: the refrigerant circuit; the cold-water loop connected to the evaporator and the hot-water loop connected to the condenser. The refrigerant circuit is composed of two fixed-speed scroll compressors working in parallel, two brazed plate heat exchangers (one working as condenser and one as evaporator) and one electronic expansion valve. The compressor model is DSG480-4 by Danfoss, designed to operate with R1234ze(E), with a swept volume flow rate equal to 222.5 m^3 h^{-1} at 50 Hz and lubricated with POE 160SZ oil. This compressor can work with the present selected refrigerants using the same lubricant oil. The evaporator and the condenser comprise 240 and 192 plates, respectively, with an associated heat transfer area of 71.2 m^2 and 56.8 m^2.
Figure 1 reports also the positioning of the sensors installed in the systems. The refrigerant temperatures are measured

with RTDs temperature sensors PT-100 (uncertainty ± 0.1 °C) while the refrigerant pressures are measured with pressure transducers (uncertainty ± 0.05% of the full scale, 45 bar). In each water circuit, RTDs PT-100 are employed to measure the temperatures at the inlet and outlet of the heat exchangers. An electromagnetic flow meter (uncertainty ± 0.25% of the measured value) is used to measure the volumetric water flow rate. A digital wattmeter (uncertainty ± 0.5 % of the measured value) registers the electric consumption of the compressors.

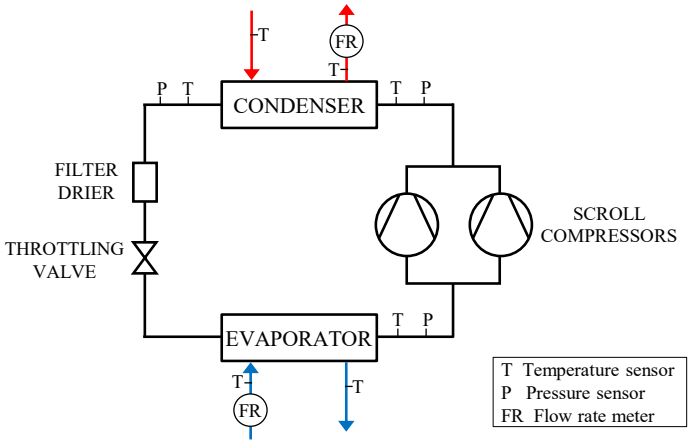

Figure 1: Layout of the test bench.

3.2 Test procedure and operative conditions

Experimental tests were conducted in steady-state conditions with one or two active compressors at defined water-side operative conditions. Steady-state conditions were achieved when the variation of condensing and evaporating pressures were within ± 0.05 bar for about 5 minutes. Once the chiller had reached steady-state conditions, the experimental data were collected over 10 minutes at a rate of one reading per second. The superheating degree at the evaporator and the subcooling at the condenser outlet were fixed at 5 K. The water temperature at the outlet of the evaporator was fixed equal to 7 °C. The water temperature at the inlet of the condenser was fixed equal to 20 °C, 30°C or 40 °C. When performing tests with two active compressors (full load), the water flow rates were set to achieve a temperature difference of 5 K in the heat exchangers. When one compressor is turned off (partial load), the water flow rates remained the same as those observed in the corresponding full load test while the temperature difference at the heat exchangers was varied. The experimental conditions of the tests performed for each refrigerant are reported in Table 2. The evaporating and condensing temperatures reached by the chiller during the experimental tests depend on the tested refrigerant. The lowest and highest values of the evaporating temperature were 2.02 °C and 4.84 °C, respectively, achieved during test 2 with R152a and R1234ze(E). With regard to the condensing temperature, the lowest values were observed with R152a during tests 1-3-5 with values equal to 22.56 °C, 32.40 °C and 42.56 °C, respectively. Conversely, the highest values were observed with R516A during tests 2-4-6 with values equal to 27.43 °C, 37.39 °C and 47.24 °C, respectively.

Additional tests with water temperatures at the inlet and outlet of the evaporator equal to 23 °C and 18 °C respectively, are presented in Conte et al. (2023).

Table 2: Experimental conditions used during the tests.

Test	Number of compressors active	Evaporator			Condenser		
		$T_{w,in}$	$T_{w,out}$	Flow rate	$T_{w,in}$	$T_{w,out}$	Flow rate
1	2	12 °C	7 °C	Determined	20 °C	25 °C	Determined
2	1	*	7 °C	as test 1	20 °C	*	as test 1
3	2	12 °C	7 °C	Determined	30 °C	35 °C	Determined
4	1	*	7 °C	as test 3	30 °C	*	as test 3
5	2	12 °C	7 °C	Determined	40 °C	45 °C	Determined
6	1	*	7 °C	as test 5	40 °C	*	as test 5

* It results from the operating conditions.

3.4 Data reduction and uncertainty analysis

The water mass flow rate is calculated by multiplying the volumetric water flow rate measured ($\dot{m}_w$) by the water density ρ_w, as follows.

$$\dot{m}_w = \frac{\dot{V}_w}{3600} \cdot \rho_w \tag{1}$$

The evaporation cooling capacity and the condenser heat flow rate are determined with an energy balance on the water side, knowing the water specific heat (c_w), the water mass flow rate and the inlet/outlet temperatures at the heat exchanger ($T_{w,in}$ and $T_{w,out}$).

$$Q_{evap} = \dot{m}_{w,evap} \cdot c_w \cdot \left(T_{w,in,evap} - T_{w,out,evap}\right) \tag{2}$$

$$Q_{cond} = \dot{m}_{w,cond} \cdot c_w \cdot \left(T_{w,in,cond} - T_{w,out,cond}\right) \tag{3}$$

The refrigerant mass flow rate can be determined from the energy balance at the condenser on the refrigerant side, knowing the inlet/outlet specific enthalpy at the condenser ($h_{r,in,cond}$ and $T_{r,out,cond}$).

$$\dot{m}_r = \frac{Q_{cond}}{h_{r,in,cond} - h_{r,out,cond}} \tag{4}$$

The volumetric efficiency of the compressor is defined as:

$$\eta_{vol} = \frac{\dot{m}_r}{N \cdot \rho_{suc} \cdot \dot{V}_{th}} \cdot 3600 \tag{5}$$

where ρ_s is the density at the compressor inlet, N is the number of compressors active and $\dot{V}_{th}$ is the theoretical swept volume flow rate equal to 222.5 $m^3\ h^{-1}$.

The compressor isentropic efficiency is defined as:

$$\eta_{comp} = \frac{\dot{m}_r \cdot \left(h_{is,disc} - h_{suc}\right)}{P_{comp}} \tag{6}$$

where ($h_{is,disc}$-h_{suc}) is the specific work for isentropic compression.

All the specific enthalpy and entropy are evaluated from the measured temperature and pressure on the refrigerant loop using Refprop 10 (Lemmon et al., 2018).

The estimation of uncertainty is done according to the ISO Guide of the Expression of Uncertainty in Measurement (Joint Committee For Guides In Measurements, 2008). The expanded combined uncertainty, obtained considering a level of confidence of about 95%, is always less than 5% for the heat flow rate at the condenser.

4. EXPERIMENTAL RESULTS AND DISCUSSION

4.1 Compressor efficiencies

Figure 2 reports the calculated values of the volumetric efficiency (Equation (5)) and of the compressor efficiency (Equation (6)) as a function of the pressure ratio (pressure at the compressor discharge divided by the pressure at the suction). The volumetric efficiency values are dispersed in a narrow interval between 0.94 and 0.99 (Figure 2a and 2b). The highest volumetric efficiency is obtained with R134a (values between 0.99 and 0.96) while for the other refrigerants, the values obtained are slightly lower, about 2%. This is due to the lower refrigerant volumetric flow rate elaborated by the compressor with the alternative refrigerants. The compressor efficiency (Figure 2c and 2d) increases with the pressure ratio and after reaching a maximum at a pressure ratio close to 3 it slightly decreases. The highest values of the compressor efficiency have been obtained with R152a and the lowest with R1234ze(E). As compared to R134a, the compressor efficiency is 2% higher for R152a and 5% lower for R1234ze(E).

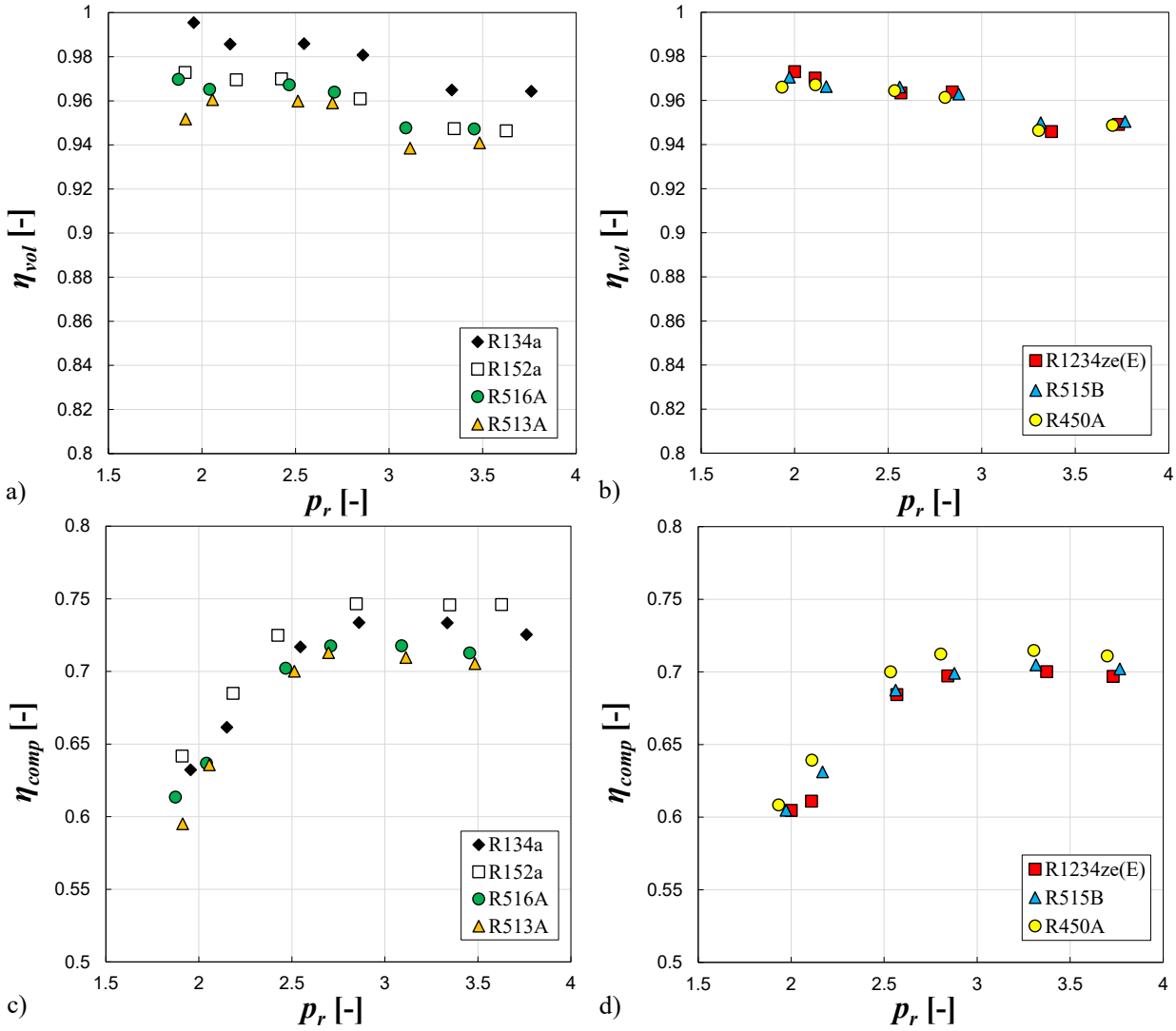

Figure 2: Volumetric efficiency (a, b) and compressor isentropic efficiency (c, d) as a function of the pressure ratio for all the refrigerants analyzed.

4.2 Compressor power consumption

Figure 3 shows the experimental data of the compressor power consumption as a function of pressure ratio, at a) full load with two compressors active and b) partial load with one compressor active. Generally, the compressor consumption increases when the pressure ratio increases, due to the higher pressure change that the compressor must provide. Considering the R134a, the compressor consumption varies from 48 kW to 73 kW with two active compressors and from 22 kW to 34 kW at partial load. Compared to R134a, all the tested refrigerants worked with lower compressor consumptions, except R516A and R513A, which have a higher compressor consumption of about 3% and 5%, respectively. The lower values were achieved with the use of R1234ze(E) and R515B, of about 22% and 25%, respectively.

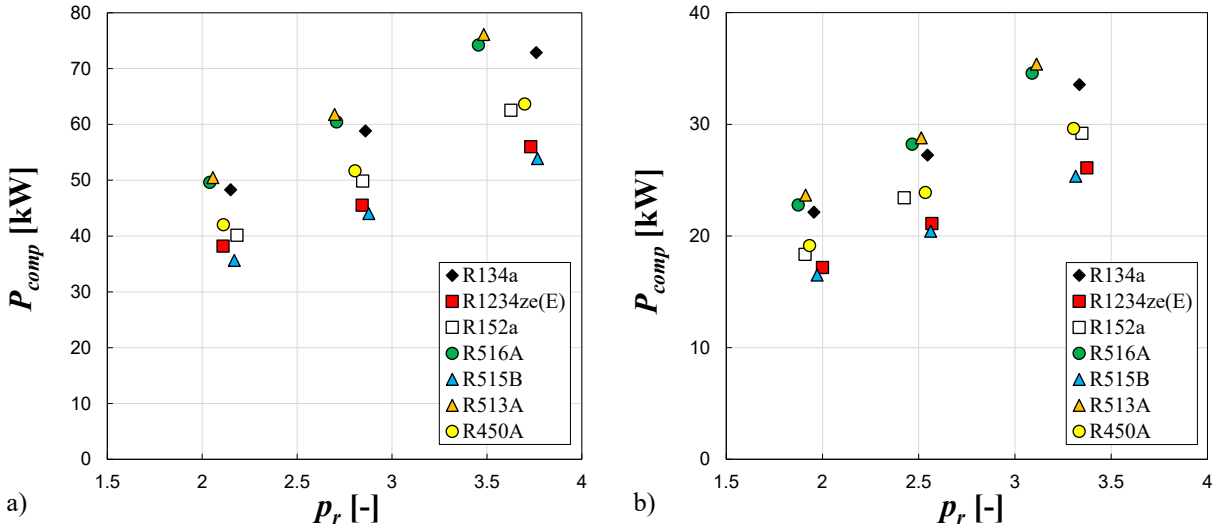

Figure 3: Compressor power consumption at a) full load (two compressors on) and b) partial load (one compressor on) as a function of the pressure ratio.

4.3 Compressor discharge temperature

Another interesting parameter when testing a compressor with various refrigerants is the discharge temperature at the compressor outlet. In fact, excessively high temperatures can reduce the lubricating effect of the oil, with possible wear effects on the moving parts of the compressor. The variation of the compressor discharge temperature as a function of pressure ratio is shown in Figure 4. The discharge temperature increases when the pressure ratio increases, due to the higher condensing pressure. Considering the R134a, at the lowest pressure ratio (about 2) the temperature is 39 °C while at the highest pressure ratio (about 3.7) it is 64 °C. Compared to R134a, R152a is the only refrigerant that has a higher compressor discharge temperature, 4 K higher at the lowest pressure ratio and 8 K higher at the highest pressure ratio. The compressor discharge temperatures for R516A, R513A and R450A have similar values that increase with pressure ratio, from 37 °C to 59 °C. The compressor discharge temperature is lower in the case of R515B: it varies from 35 °C to 56 °C.

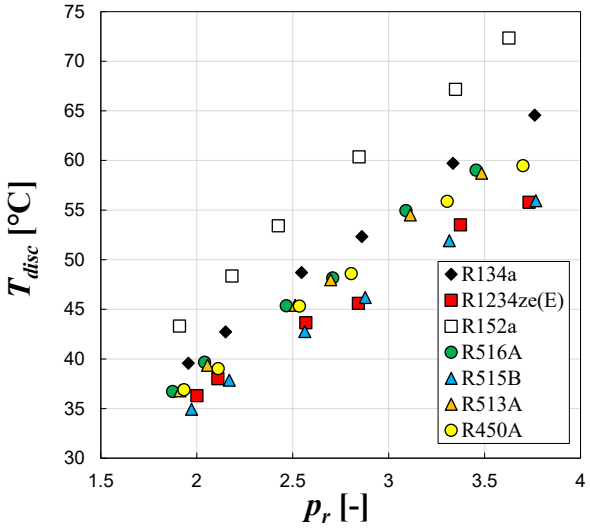

Figure 4: Compressor discharge temperature as a function of the pressure ratio.

5. CORRELATION TO PREDICT THE COMPRESSOR EFFICIENCIES

The experimental data of the compressor efficiencies have been compared to the values calculated by the correlations developed by Pierre (1982) and Navarro et al. (2013). Pierre suggested two equations with a lower number of parameters compared to the AHRI polynomials (AHRI, 2020) for open piston compressors working with R714, R12, R22 and R502. In the Pierre correlation, the volumetric efficiency η_{vol} and the efficiencies ratio η_{vol}/η_{comp} are calculated with the following equations:

$$\eta_{vol} = k_1 \cdot \left(1 + \frac{t_{suc} - 18}{100} \cdot k_s\right) \cdot e^{k_2 \cdot R_p} \tag{7}$$

$$\frac{\eta_{vol}}{\eta_{comp}} = k_1' \cdot \left(1 + \frac{t_{suc} - 18}{100} \cdot k_2'\right) \cdot e^{aR_T + b} \tag{8}$$

where t_s is the suction compressor temperature in [°C], R_p is the pressure ratio, R_T is the temperature ratio between the condensing and the evaporating temperature in [K] and k_1, k_2, k_s, k_1', k_2', a and b are empirical coefficients depending on the refrigerant.

Navarro et al. (2013) performed an experimental study with one scroll compressor (swept volume equal to 35 $cm^3\,rev^{-1}$) with propane (R290). Their results show that Pierre correlation can reproduce the behaviour of the volumetric efficiency but fail in the prediction of the efficiencies ratio. Thus, Navarro et al. proposed new values for the coefficients used in the Pierre correlation, obtained with a fitting of their data and suggested the use of two new non-dimensional parameters (the "non-dimensional mass flow rate" and "non-dimensional power consumption"). The "non-dimensional mass flow rate" differs from the volumetric efficiency by replacing the vapor density at suction with the saturated vapor density at the same pressure:

$$\dot{m}' = \frac{\dot{m}_r}{\rho_{sat} \cdot \dot{V}_{theor}} \cdot 3600 \tag{9}$$

and it can be evaluated with the following equation:

$$\dot{m}' = k_1 \cdot \left[1 - F\left(\frac{SH}{T_{sat}}\right)\right] \cdot e^{k_2 \cdot R_p} \tag{10}$$

where T_{sat} and ρ_{sat} are respectively temperature (in [K]) and density at saturated conditions, SH is the superheat, F is a constant, k_1 and k_2 are two empirical coefficients. The parameter $\dot{m}'$ calculated with Equation (10) is then used to evaluate the refrigerant mass flow rate and consequently the volumetric efficiency with Equation (5).

The "non-dimensional power consumption" parameter is defined as:

$$E' = \frac{P_{comp}}{p_{suc} \cdot \dot{V}_{theor}} \cdot 3600 \tag{11}$$

and it can be evaluated with the following equation:

$$E' = \frac{1}{k_1' + k_2' \cdot e^{k_3' \cdot R_p}} \tag{12}$$

where k_1', k_2' and k_3' are three empirical coefficients. The parameter E' calculated with Equation (12) allows to estimate the power consumption of the compressor and consequently the compressor efficiency with Equation (6).

Regarding the coefficients reported in Equations 7-8-10-12, the values reported in Navarro et al. (2013) for a scroll compressor working with R290 have been considered. These correlations can accurately estimate the volumetric efficiency of the present scroll compressor, but the compressor isentropic efficiency is underestimated by an error of about 20% for Pierre correlation and 65% for the Navarro et al. It is important to notice the reasons for the discrepancy between the experimental and the calculated compressor isentropic efficiency. In the present study, the refrigerants considered are R134a, R1234ze(E), R152a, R516A, R515B, R513A, and R450A which were not included in the Navarro et al. database and the swept volume of the present scroll compressor is equal to 1268 $cm^3\,rev^{-1}$, about 36 times larger than the compressor used by Navarro et al. The compressor size, as reported by Navarro et al. (2013), can affect the k_3' coefficient while the k_1' coefficient can be affected by the refrigerant used. Therefore, to better predict the compressor efficiencies, the present database has been used to determine new values for the parameters needed in the Pierre correlation and in the Navarro et al. correlation. The new values obtained from the present data are reported in Table 3 with the corresponding correlation factor R^2.

Table 3: New parameters of correlations for scroll compressors using the refrigerants tested in the present study.

Volumetric efficiency parameters for Pierre correlation				
k_1	k_2	k_s		R^2
0.9988	-0.01067	-0.01417		0.4537
Efficiency ratio parameters for Pierre correlation				
k_1'	k_2'	a	b	R^2
1	0	-2.391	3.01	0.81
Nondimensional mass flow rate parameters for Navarro et al. correlation				
k_1	k_2	F		R^2
0.9841	-0.01277	0.75		0.4157
Nondimensional compressor power consumption parameters for Navarro et al. correlation				
k_1'	k_2'	k_3'		R^2
0.4199	2.29	-0.7411		0.99

Figure 5 shows the comparison between the experimental and numerical results when considering the ratio between the volumetric and the compressor efficiency calculated with the Pierre and the Navarro et al. correlations using the new coefficients (reported in Table 3). Both correlations with the new coefficients estimate with good accuracy the efficiency ratio: the Pierre correlation slightly overestimates the experimental data with a maximum error of equal to 8%; the Navarro et al. correlation slightly underestimates the experimental data with a maximum error equal to 7%.

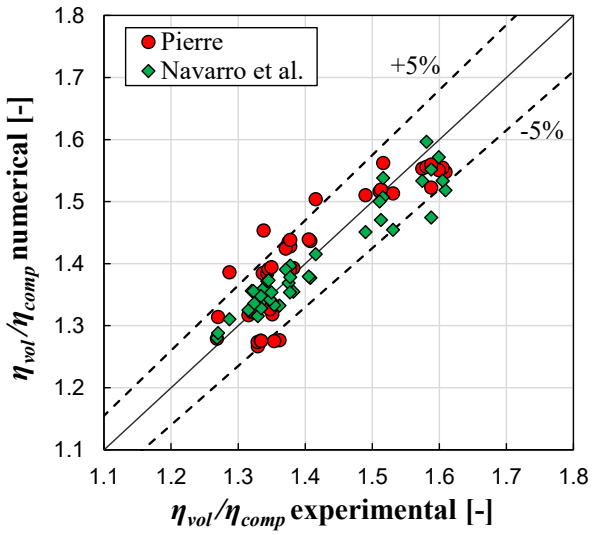

Figure 5: Comparison between the experimental and the calculated efficiency ratio using the Pierre and the Navarro et al. correlations with the new coefficients reported in Table 3 and obtained from the present database.

6. CONCLUSIONS

In this work, experimental tests have been conducted on a water-to-water vapor compression system equipped with two scroll compressors working in parallel to study the compressor performance of several refrigerants considered as possible low-GWP alternatives to R134a. The swept volume for each compressor is equal to 222.5 $m^3\ h^{-1}$.
Tests have been conducted when producing chilled water with R134a, R1234ze(E), R152a, R516A, R515B, R450A and R513A under the same water-side working conditions. The main results are reported in the following.

- The highest compressor volumetric efficiency values have been achieved with R134a (range between 0.99 and 0.96) while the other refrigerants present values lower by 1-2% compared to R134a. The highest compressor isentropic efficiency values have been obtained with R152a (on average 2% higher than those of R134a) while for the other refrigerants the values are from 1 to 5% lower.

- Regarding the compressor power consumption, all the refrigerants tested worked with a lower compressor consumption compared to R134a, except for R516A and R513A, which are higher by about 3% and 5%, respectively.
- During the experimental tests, the compressor discharge temperature with R134a increases from 39 °C to 64 °C when increasing the condensing temperature. The refrigerant R152a is the only one that has a higher compressor discharge temperature compared to R134a, while the lowest values are achieved with R515B.
- The experimental data collected have been used to assess the accuracy of Pierre (1982) and Navarro et al. (2013). New coefficients have been determined from the data regression of the present database. The values of efficiency ratio of volumetric to isoentropic efficiency are predicted with a maximum error equal to 8% by the Pierre correlation and equal to 7% by the Navarro et al. correlation. These results are particularly interesting considering the lack of data on scroll compressors operating with medium-low pressure refrigerants.

NOMENCLATURE

c	specific heat	(J kg^{-1} K^{-1})
h	specific enthalpy	(J kg^{-1})
$\dot{m}$	mass flow rate	(kg s^{-1})
N	number of compressors	(–)
ρ	density	(kg m^{-3})
P	electrical power	(W)
p	pressure	(bar)
Q	heating capacity	(W)
η	efficiency	(–)
s	specific entropy	(J kg^{-1} K^{-1})
T	temperature	(K)
t	temperature	(°C)
$\dot{V}$	volumetric flow rate	(m^3 h^{-1})

Subscript

comp	compressor
cond	condenser
disc	discharge
evap	evaporator
r	refrigerant
suc	suction
th	theoretical
vol	volumetric
w	water

REFERENCES

AHRI. (2020). *Standard 540: Performance Rating of Positive Displacement Refrigerant Compressors*.

Al-Sayyab, A. K. S., Navarro-Esbrí, J., Barragán-Cervera, A., Kim, S., & Mota-Babiloni, A. (2022). Comprehensive experimental evaluation of R1234yf-based low GWP working fluids for refrigeration and heat pumps. *Energy Conversion and Management*, *258*(November 2021). https://doi.org/10.1016/j.enconman.2022.115378

Bell, I. H., Domanski, P. A., McLinden, M. O., & Linteris, G. T. (2019). The hunt for nonflammable refrigerant blends to replace R-134a. *International Journal of Refrigeration*, *104*, 484–495. https://doi.org/10.1016/J.IJREFRIG.2019.05.035

Colombo, L. P. M., Lucchini, A., & Molinaroli, L. (2020). Experimental analysis of the use of R1234yf and R1234ze(E) as drop-in alternatives of R134a in a water-to-water heat pump. *International Journal of Refrigeration*, *115*, 18–27. https://doi.org/10.1016/j.ijrefrig.2020.03.004

Conte, R., Azzolin, M., Bernardinello, S., & Del Col, D. (2023). Experimental investigation of large scroll compressors working with six low-GWP refrigerants. *Thermal Science and Engineering Progress*, *44*, 102043. https://doi.org/10.1016/J.TSEP.2023.102043

EU No 2024/573. (2024). Regulation (EU) 2024/573 of the European Parliament and of the Council of 7 February 2024 on fluorinated greenhouse gases, amending Directive (EU) 2019/1937 and repealing Regulation (EU) No 517/2014. *Off. J. Eur. Union*.

IPCC. (2022). IPCC, 2022: Climate Change 2022: Mitigation of Climate Change. Contribution of Working Group III to the Sixth Assessment Report of the Intergovernmental Panel on Climate Change. In *The Daunting Climate Change*. https://doi.org/10.1017/9781009157926

Joint Committee For Guides In Measurements. (2008). Evaluation of measurement data — Guide to the expression of uncertainty in measurement. *International Organization for Standardization Geneva ISBN*. https://doi.org/10.1373/clinchem.2003.030528

Lemmon, E. W., Bell, I. H., Huber, M. L., & McLinden, M. O. (2018). *NIST Standard Reference Database 23: Reference Fluid Thermodynamic and Transport Properties-REFPROP, Version 10.0, National Institute of Standards and Technology*. https://www.nist.gov/srd/refprop

Llopis, R., Sánchez, D., Cabello, R., Catalán-Gil, J., & Nebot-Andrés, L. (2017). Experimental analysis of R-450A and R-513A as replacements of R-134a and R-507A in a medium temperature commercial refrigeration system. *International Journal of Refrigeration*, *84*, 52–66. https://doi.org/10.1016/j.ijrefrig.2017.08.022

Makhnatch, P., Mota-Babiloni, A., López-Belchí, A., & Khodabandeh, R. (2019). R450A and R513A as lower GWP mixtures for high ambient temperature countries: Experimental comparison with R134a. *Energy*, *166*, 223–235. https://doi.org/10.1016/j.energy.2018.09.001

Mendoza-Miranda, J. M., Mota-Babiloni, A., Ramírez-Minguela, J. J., Muñoz-Carpio, V. D., Carrera-Rodríguez, M., Navarro-Esbrí, J., & Salazar-Hernández, C. (2016). Comparative evaluation of R1234yf, R1234ze(E) and R450A as alternatives to R134a in a variable speed reciprocating compressor. *Energy*, *114*, 753–766. https://doi.org/10.1016/j.energy.2016.08.050

Mota-Babiloni, A., Makhnatch, P., Khodabandeh, R., & Navarro-Esbrí, J. (2017). Experimental assessment of R134a and its lower GWP alternative R513A. *International Journal of Refrigeration*, *74*, 680–686. https://doi.org/10.1016/j.ijrefrig.2016.11.021

Mota-Babiloni, A., Navarro-Esbrí, J., Barragán, Á., Molés, F., & Peris, B. (2014). Drop-in energy performance evaluation of R1234yf and R1234ze(E) in a vapor compression system as R134a replacements. *Applied Thermal Engineering*, *71*(1), 259–265. https://doi.org/10.1016/j.applthermaleng.2014.06.056

Navarro-Peris, E., Corberán, J. M., Falco, L., & Martínez-Galván, I. O. (2013). New non-dimensional performance parameters for the characterization of refrigeration compressors. *International Journal of Refrigeration*, *36*(7), 1951–1964. https://doi.org/10.1016/j.ijrefrig.2013.07.007

Pierre, B. (1982). *Kylteknik, Allma¨n Kurs. Inst. Mekanisk Va¨ Rmeteori Och Kylteknik. KTH, Stockholm (in Swedish)*.

Sánchez, D., Cabello, R., Llopis, R., Arauzo, I., Catalán-Gil, J., & Torrella, E. (2017). Évaluation de la performance énergétique du R1234yf, du R1234ze(E), du R600a, du R290 et du R152a comme alternatives à faible GWP au R134a. *International Journal of Refrigeration*, *74*(2017), 267–280. https://doi.org/10.1016/j.ijrefrig.2016.09.020

Amendment to the Montreal Protocol on Substances that Deplete the Ozone Layer (Kigali Amendment), (2016).

ACKNOWLEDGEMENT

Danfoss is acknowledged for the information provided on the scroll compressor. Swegon Operations S.r.l. is acknowledged for manufacturing the apparatus used in the experimental tests.